Assessing the Impacts of Land Use Diversity on Urban Heat Island in New Cities in Egypt, Tiba City as a Case Study

Dr. Omar Hamdy
> Assistant Professor-Faculty of Engineering-Aswan University, omar.hamdy@aswu.edu.eg

Eng. Zeinab A. Alsonny
> Master student-Faculty of Engineering-Aswan University, engzeinababdallah@gmail.com

Abstract:

Egypt had two problems: population growth and population concentration, which were solved by moving to new cities. Rapid urbanization and changing lifestyles have disrupted the ecological structure of cities. This has given rise to the phenomenon of urban heat islands (UHI). This phenomenon is characterized by higher air and surface temperatures in cities than in rural areas. The research into this phenomenon is based on land surface temperatures (LST), which are closely related to land use characteristics (LU). Researchers can now measure LST across wide areas with great temporal and spatial accuracy using remote sensing (RS), Geographical information systems (GIS), and statistical approaches. Google Earth's high-resolution maps also help identify LU classes. All of these assisted in achieving the study's main goal of examining the impact of LU on LST and hence the phenomena of UHI in new cities. The LU diversity was determined using high-resolution Google Earth maps, while the LST was extracted using free RS data. The study concluded that paved and unpaved roads, as well as unoccupied places, absorb considerable amounts of solar radiation, leading to increased heat storage and UHI. The coldest temperatures were reported in residential and green regions.

1. Introduction:

Egypt had two major issues: the problem of rapid population growth, which caused urban sprawl in agricultural areas (Hamdy et al. 2014), and the problem of a significant concentration of population and activities in a limited region of the map that barely exceeded 4% of Egypt's total territory. For example, the annual loss of agricultural land in some Cairo districts exceeds 15% (M. Salem et al. 2020), and 29 agricultural plots were converted to residential buildings until 2016 (Osman et al. 2016). So the solution was to head to the Egyptian desert and coast in order to create new cities (E. O. Salem and Monir 2017). It aims to accommodate the increasing demand for housing and provide an opportunity to loosen the focus around the narrow Nile Valley and redraw the urban map of Egypt (Ibrahim and Masoumi 2016). The policy of establishing new cities was launched in the seventies of the last century, with the establishment of the Tenth of Ramadan City as the first new Egyptian city, and then the New Urban Communities Authority took over the establishment of the new cities (Hegazy and Moustafa 2013). So far, over 50 new cities have been constructed in Egypt, divided into four generations. This helped to reduce encroachment on agricultural areas, provide dwellings for various parts of society, and create work possibilities by creating numerous industrial facilities (Ellahham 2014). Urban expansion, on the other hand, entails more impermeable constructed surfaces(Liu et al. 2021), which may have an

impact on air quality and urban climate (Wang et al. 2020), (Robbiati et al. 2022), (Unal Cilek and Cilek 2021).

The urban heat island phenomenon (UHI) is regarded to be one of the most important factors influencing the urban climate (Bahi, Mastouri, and Radoine 2020). This phenomenon is one of the most serious challenges facing humans in the twenty-first century, and it is a result of the urbanization and industrialization of human society (Memon, Leung, and Chunho 2008). It is a phenomenon that has a negative impact on cities, and is characterized by an increase in air and surface temperatures in cities when compared to rural areas (Shafiee et al. 2020), (Chen, Shan, and Yu 2022), (Yin et al. 2019), (Voogt and Oke 2003). UHI has been shown to have a deleterious impact on the health and thermal comfort of city dwellers (Zhang et al. 2021), (Liu et al. 2021), (Taripanah and Ranjbar 2021), (Stache et al. 2021). Because they are subjected to higher temperatures than residents of the surrounding area (Zou et al. 2021). Increased temperatures exacerbates human heat stress by reducing the effectiveness of convection, conduction, and cutaneous perspiration in cooling the body (Huang et al. 2021), (Wu et al. 2021). During hot summers, this leads to an increase in the rate of heat-related disorders and an increase in the death rate (Zou et al. 2021), (Zhang et al. 2021). As a result, residents have resorted to excessive energy consumption in buildings to avoid the effects of high temperatures in an attempt to cool down and

obtain thermal comfort, which has the opposite effect of increasing the external temperature and thus exacerbating UHI (Huang et al. 2021), (Mushore, Odindi, Dube, and Mutanga 2017), (Tran et al. 2017), (Zhang et al. 2021), (Santamouris 2014).

UHI occurs primarily as a result of changes in urban surfaces and an increase in the area of concrete and asphalt surfaces, which results in increased thermal storage capacity and thermal conductivity. Which contributed to the increase in LST and amplification of the UHI phenomenon (Shafiee et al. 2020), (Yin et al. 2019). In climate change research, the land surface temperature (LST) has been frequently used as a UHI indicator, as it is a key variable (Stroppiana, Antoninetti, and Brivio 2014), (Tran et al. 2017), (Weng 2009). Experts have researched some possible solutions to reduce UHI (Memon, Leung, and Chunho 2008). Such as increasing greening (Yang et al. 2017), (Haq 2011), increased albedo of city rooftops, and other measures and recommendations (Stache et al. 2021). However, directly applying the planned city-wide mitigating measures to all blocks with various forms of land use (LU) is difficult (Zou et al. 2021). LST has a direct relationship with the LU characteristics of the urban area (Weng 2009). It is therefore necessary to consider the relationship between LU and LST to understand how LU affects UHI (Tran et al. 2017). Previous research has shown that the spatial structure of impermeable surfaces, water gaps, and vegetation cover all have a direct impact on LST (Mushore, Odindi, Dube, and Mutanga 2017). Studies have also revealed that the influence of buildings and vegetation on UHI is dependent on the density of the structures and vegetation cover (Mushore, Odindi, Dube, Matongera, et al. 2017). The number of impermeable materials that can store heat is one of the indicators of UHI (Ulfiasari and Yola 2022). As well as human activities have a significant impact on long-term surface temperature (Weng 2009). Thus understanding how LU affects LST will substantially assist planners in making decisions that will reduce their UHI impact (Taripanah and Ranjbar 2021).

Google Earth, as a reliable source of location data, may be used for accurate verification, mapping, and preliminary research, and it is freely available to anybody interested in maps (Ragheb and Ragab 2015). Because of the great resolution of these photos, observers can easily discern between different land cover classes and distinguish different components of the built environment, such as industrial plants and individual dwellings, as well as different roads (Hamdy et al. 2016),

(HAMDY and ZHAO 2016). Google Earth Maps also features a date range from 2000 to the present allowing LU mapping to earlier years. It also has enough spatial and chromatic detail to distinguish real-world objects. In the Google Earth desktop application, several recent studies used Manual photointerpretation of high-resolution images as reasonably accurate, low-cost reference data for producing LU maps and testing their accuracy (Hamdy et al. 2016).

Ground measurements cannot provide data for large areas of land due to the difficulty of conducting LST measurements in the field. Satellites have made it feasible to measure LST with suitable geographical and temporal precision all over the world, as well as comprehensive spatial data rather than point values, thanks to the introduction of remote sensing (RS) technologies from space (Li et al. 2013). RS is nowadays an indispensable source of information about the LST and the quasi-continuous surface observation of the UHI (Kulo 2018), (Bechtel, Zakšek, and Hoshyaripour 2012). Geographical information systems (GIS) and statistical methodologies have also assisted researchers in describing and investigating the link between UHI and LU (Tran et al. 2017). GIS can analyze, combine, and manipulate geographic data on the surface or beneath it. Using it and remote sensing together can assist find the optimal sites for urban growth (Youssef, Pradhan, and Tarabees 2011).

The primary objective of the research is to investigate the effect of LU diversity on LST and its reflection on UHI in New Tiba as a case study of new cities in Egypt using free and accessible data. The main objective can be achieved from two sub-goals. The first goal is to create a map of different types of LU using free and trusted sources like Google Earth. The second objective is to extract the city's LST using freely available remote sensing data and GIS. Achieving these stated goals will provide a robust methodology using inexpensive data that can assist urban planners in developing countries in researching the impacts of LU on UHI.

2. The Study Area:

The new city of Tiba was initiated by Republican Decree No. 198 of the year 2000 AD. Located 14 kilometers northeast of Luxor and 10 kilometers from Luxor International Airport (Fig. 1), the city is a popular tourist destination. According to Resolution No. 329 of 2014, the overall land area of the city is 9,496 acres, which includes an additional 4,050 acres that were added to the city limits. When measured in acres (Fig. 2), the current urban area is 2,431 acres, which is divided into six residential neighborhoods. Service areas covering a total area

of 1509 acres are located in the center of them. In addition, there is a 382-acre industrial park. It includes an investment land area, universities, and the central services area, among other things, with a

total land size of 540 acres ("New Urban Communities Authority, Home Page - New Tiba," n.d.).
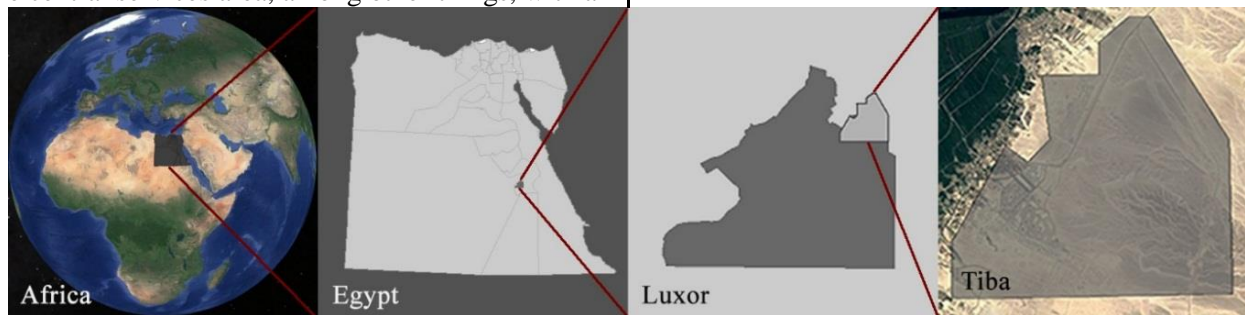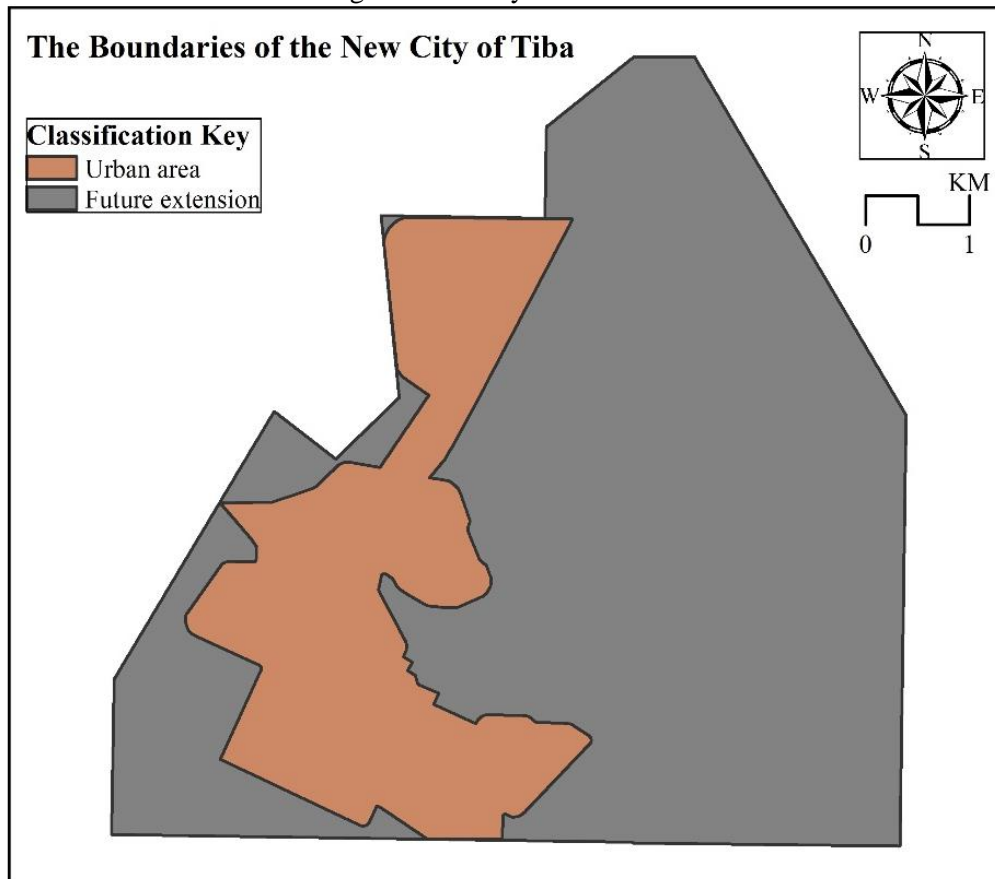

Fig. 1. The study area location.

Fig. 2. The Boundaries of the New City of Tiba.

3. Research Methodology:

Multiple methodologies were used in the process of conducting this research, which was carried out in several stages. The inductive method was used to gather information on the city and the uses of urban area. The New Tiba City Authority provided the relevant maps and coordinates for this research work. The previous data was used in conjunction with Google Earth and GIS to create a map of urban LU with the applied approach. Satellite images were processed using LST extraction equations, and the resulting temperatures were classified. Analytical methods were utilized to investigate the link between LST and LU in order to better understand the influence of different

usages on UHI.

3.1. The Stage of Mapping the Urban Area LU

A field trip to the newly established city of Tiba was organized. The New Tiba City Authority provided an AutoCAD map of the entire city, which included all uses, extensions, and locations of the city. This information was used to categories the uses of urban space into eight main categories: residential, service, under construction, green, urban space gaps, empty areas, paved and unpaved roads it was necessary to create a LU map of the urban area on the GIS software, which was based on the manual interpretation of Google Earth maps of 2019.

3.2. LST Extraction Stage for the City

LST was extracted for three satellite images on 6/26, 7/28 and 8/29 of 2019. LST was averaged over the summer months. Satellite images of Landsat 8 were obtained from the USGS(United States Geological Survey) website: https://earthexplorer.usgs.gov/(USGS n.d.). The LST was obtained by applying some equations to satellite images (Table 1). The sequence of LST extraction equations begins by converting digital image values into satellite spectral irradiance values via equation (1). Followed by the stage of calculating the absolute temperature, or the so-called black body temperature at the satellite in Kelvin, through equation (2). Then the temperature in Kelvin is converted to Celsius temperature by equation (3).

This method of extracting LST was based on the calculation of the NDVI (Normalized Differential Vegetative Index): a simple graphical or numerical indicator that expresses the intensity of greening. It is used to analyze RS measurements, and it can be calculated by equation (4). Then the percentage of this vegetation cover is calculated using equation (5), as well as calculating the emission through equation (6). Finally, the LST is calculated by equation (7), depending on the NDVI and the black body temperature at the satellite as well as the emissivity (which was calculated previously). These equations are performed on heat bands 10 and 11 and their values are averaged.

Table 1. Equations for extracting LST.

	Equation	Symbols meaning	References
(1)	$L\lambda = ML * QCAL + AL$	Lλ = Spectral Radiance at the sensor's aperture, ML = Band-specific multiplicative rescaling factor from the metadata, AL= Band-specific additive rescaling factor from the metadata, Qcal = Quantized calibrated pixel value in DNs.	(Abdu Yaro, Lawal Abdulrashid 2017), (Asgarian, Amiri, and Sakieh 2015)
(2)	$T_{(K)} = \dfrac{K2}{\ln\left(\dfrac{K1}{L\lambda} + 1\right)}$	Lλ= Spectral Radiance at the sensor's aperture, K1, K2= Calibration constants (from metadata files). Its values changed according to the satellite.	(Abdu Yaro, Lawal Abdulrashid 2017), (Sekertekin and Bonafoni 2020), (Mushore, Odindi, Dube, and Mutanga 2017), (Giannini et al. 2015)
(3)	$T_{(°C)} = T_{(K)} - 273.15$	T(K)= Temperature in kelvins.	(Al-Jashami 2018)
(4)	$NDVI = (Band5 - Band4)/(Band5 + Band4)$	**Band5**= Near infrared bands, **Band4**= Visible infrared bands.	(Abdu Yaro, Lawal Abdulrashid 2017), (Giannini et al. 2015), (Yu, Guo, and Wu 2014)
(5)	$P_V = \left(\dfrac{NDVI - NDVI_{MIN}}{NDVI_{MAX} - NDVI_{MIN}}\right)^2$	NDVImin =Minimum value of NDVI, NDVImax =Maximum value of NDVI.	(Abdu Yaro, Lawal Abdulrashid 2017), (Sekertekin and Bonafoni 2020), (Giannini et al. 2015)
(6)	$\varepsilon = 0.004P_V + 0.986$	Pv = Percentage of vegetation.	(Abdu Yaro, Lawal Abdulrashid 2017)
(7)	$LST = \dfrac{T_{(°C)}}{1 + \left(\dfrac{L\lambda * T_{(°C)}}{\rho}\right) * \ln(\varepsilon)}$	ρ =Constant value $= h * \dfrac{c}{\sigma} = (1.438 * 10^{-2} m * K)$	(Giannini et al. 2015)

3.3. The Stage of Studying the Relationship between LST and LU

The LST extracted from the RS data was distributed over the urban area LU of the city to study the relationship between them. To achieve this, the average, maximum, and minimum LST values for each LU element were determined during each summer month. The average LST of the total summer months was also calculated for all LU elements. These values were studied to reach a clear relationship between LST and LU.

4. Results and Discussion:

As part of the study's defined methodology, a LU map of the urban area was created, as well as the LST for the summer months and the average between the three months. In order to attempt to understand the relationship between LU and LST, the maximum and minimum values of LST during the summer months were determined for LUs throughout the summer months. It was also discovered what the average LST was throughout the summer months and how it was linked to the LUs and their surrounding area.

4.1. Urban Area LU

The LU map of urban area shows that most of the urban area is still empty areas as shown in Fig. 3 and Fig. 4. The area of the empty areas is approximately 930 acres (38%). It is followed in the area by the gaps and unpaved roads, and their areas are 696(29%) and 300(12%) acres,

respectively. The areas of the remaining uses varied as shown in Table 2. The service use was the least in terms of area, and its area reached approximately 32(1%) acres.
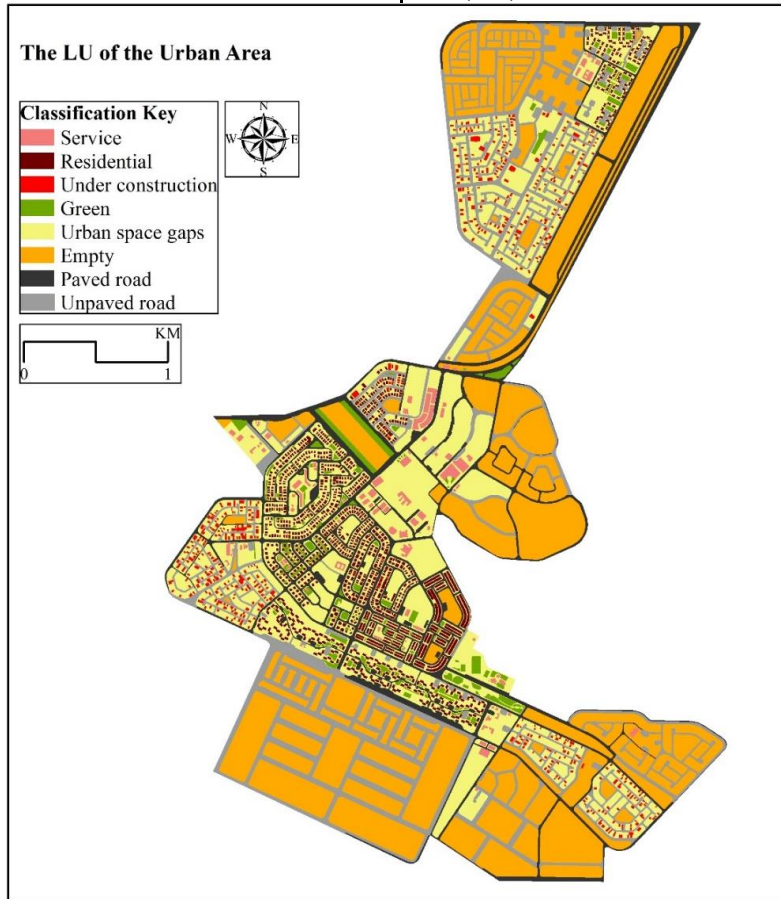

Fig. 3. LU of the urban area.

Table 2. The area of LU and their percentage

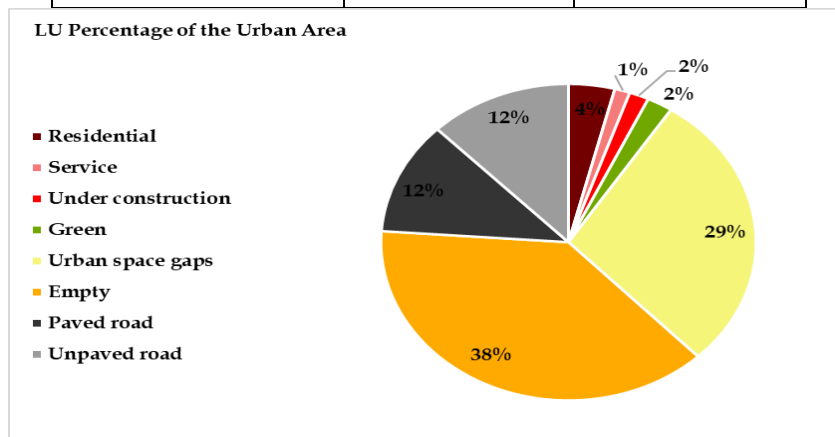| LU	Area (acres)	Percentage
Residential	96.7	4%
Service	32.3	1%
Under construction	41.0	2%
Green	54.1	2%
Urban space gaps	696.7	29%
Empty	930.3	38%
Paved road	281.0	12%
Unpaved road	300.0	12%
Total	2432.1	100%

Fig. 4. LU percentage for urban area.

4.2. LST for Urban Area

During the summer months, three separate satellite images were used to extract urban space area LST, as shown in Fig. 5. The warmest temperatures were recorded during LST in June. Temperatures ranged from 40 to nearly 46 °C in it, on average. However, the LST for July was the coolest during the summer, with temperatures ranging from 38 to 44 °C on a daily basis. Afterwards, the LST began to rise gradually in August, with temperatures ranging from 38 to 46 degrees. The average temperature of the urban environment fluctuated between 39 and 45 ° C throughout the summer of 2019 as a result (Fig. 6).
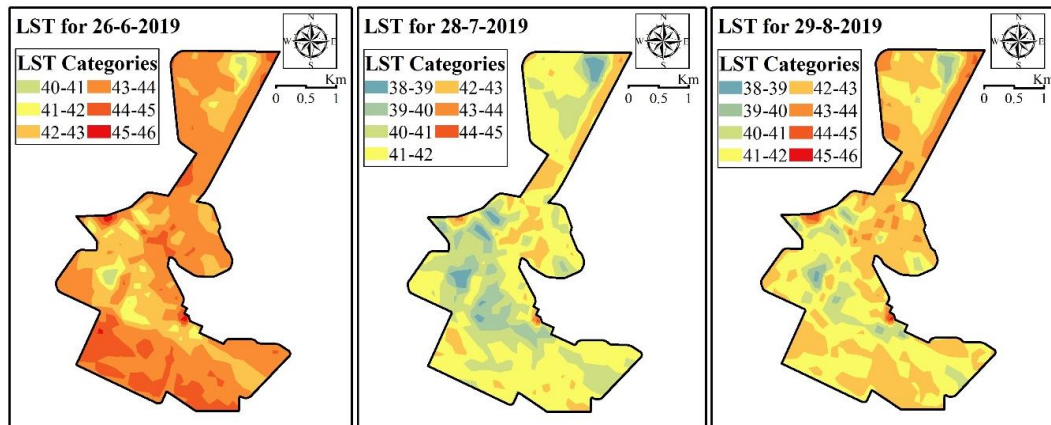

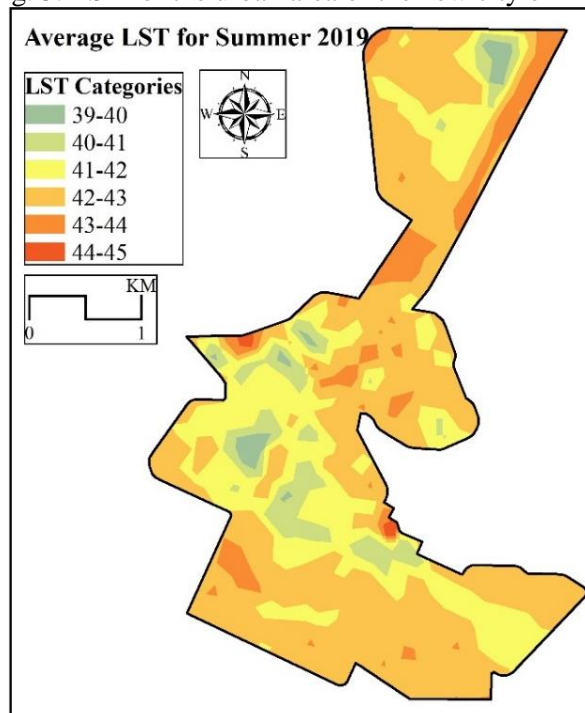Fig. 5. LST for the urban area of the new city of Tiba.

Fig. 6. Average LST for summer 2019.

4.3. Relationship between LST and LU

LST were distributed over the LU of the urban area. Then the LST values for all LU were compared as in **Error! Reference source not found.**. The comparison was carried out in two parts as follows:
4.3.1. Max and Min LST Value for LU: Fig. 7 shows the max values of LST for LU during the summer months of 2019. The max values of LST recorded for residential use for the months of June, July and August were the lowest values recorded. They are equal to 43.70, 41.91 and 42.71 °C, respectively, with an average of 42.77 °C. While the max values of LST for green spaces reached 45.76, 44.30 and 45.07 °C, respectively, which are the highest values recorded during the summer months of 2019 with an average of 45.04 °C. This comparison is clearly shown in Fig. 9.

The min LST values for all LU are shown in Fig. 8. The lowest values were recorded for urban gaps during the summer months. The average min values recorded for urban space gaps for the summer months were 39.03 °C. While the min value recorded for the buildings under construction was the highest in the values, with an average of 40.86 °C, as shown in Fig. 10.

Table 3. LST for LU of the urban area.

|		June	July	August	Average
Residential	Max value	43.70	41.91	42.71	42.77
	Min value	40.49	38.03	38.79	39.10
	Average value	42.31	39.98	40.99	41.09
Service	Max value	44.00	42.34	43.11	43.15
	Min value	40.63	38.15	39.09	39.29
	Average value	42.86	40.87	41.70	41.81
Under construction	Max value	43.95	41.78	43.18	42.97
	Min value	42.01	39.87	40.71	40.86
	Average value	43.12	41.01	41.93	42.02
Green	Max value	45.76	44.30	45.07	45.04
	Min value	40.47	38.04	38.73	39.08
	Average value	42.19	39.95	40.92	41.02
Urban space gaps	Max value	45.64	43.81	44.64	44.69
	Min value	40.35	38.02	38.72	39.03
	Average value	42.98	40.88	41.78	41.88
Empty	Max value	45.38	43.16	44.60	44.38
	Min value	41.35	39.03	40.34	40.24
	Average value	43.66	41.50	42.26	42.47
Paved road	Max value	45.24	43.13	44.46	44.28
	Min value	40.36	38.03	38.78	39.06
	Average value	43.07	40.98	41.92	41.99
Unpaved road	Max value	45.14	42.82	44.25	44.07
	Min value	40.61	38.45	39.69	39.58
	Average value	43.47	41.20	42.02	42.23
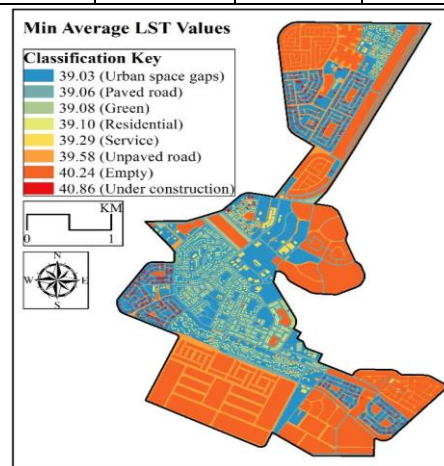
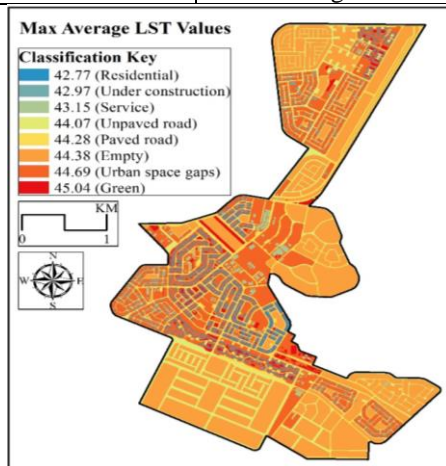
Fig. 7. The max average LST values in summer 2019. Fig. 8. The min average LST values in summer 2019.
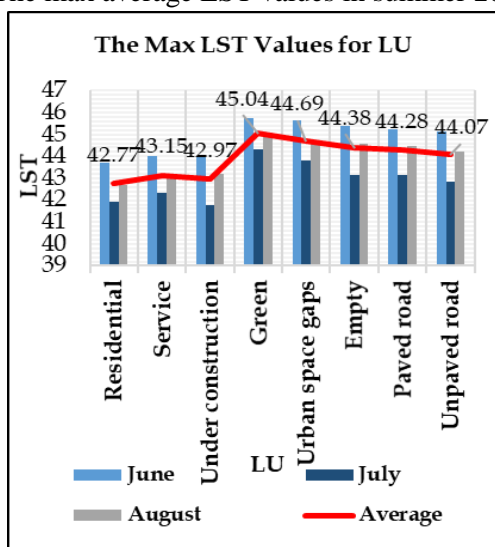

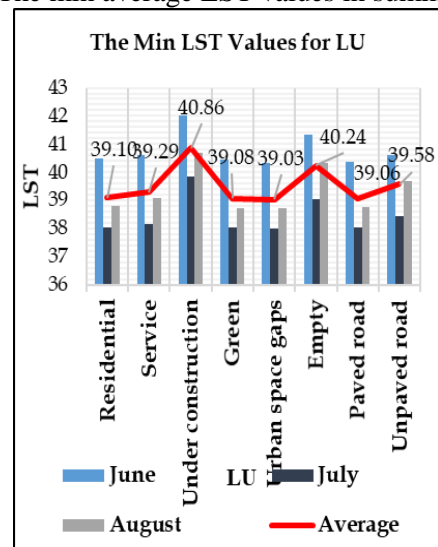Fig. 9. The max LST values for LU.   Fig. 10. The min LST values for LU.

4.3.2. Average LST of Urban Area LU:

The average LST for each summer month was compared in Fig. 11. The comparison showed that the average LST of empty areas were the highest in values for June, July and August, corresponding to 43.66, 41.5 and 42.26 ℃, respectively. While residential use and green spaces were the lowest in the LST average and the most close between them. The average LST for residential use and green spaces in June was 42.31 and 42.19 ℃, respectively. While the LST average in July was 39.98 and 39.95 ℃, respectively. In August, it is equal to 40.99 and 40.92 ℃, respectively.

By comparing the area with the average LST for LU in. It is clear that green areas and residential use

are the lowest in the average temperature, equivalent to 41.02 and 41.09 ℃, respectively. However, their area is small in comparison to the empty areas, paved and unpaved roads, which amounted to 930, 281 and 300 acres, respectively. Their average LST was 42.47, 41.99 and 41.23 ℃, respectively, which had an effect on raising temperatures in urban space gaps, which amounted to 41.88 ℃ more than the effect of lowering temperatures in residential and green areas. This caused an increase in the average LST of the total urban area, which amounted to 42.11 ℃. This also means UHI elevation of urban area. This difference is clearly shown in Fig. 12.

Table 4. The area of LU and their average LST.

LU	Area (acres)	Average summer LST
Residential	96.8	41.09
Service	32.3	41.81
Under construction	50	42.02
Green	54.1	41.02
Urban space gaps	696.8	41.88
Empty	930.3	42.47
Paved road	281	41.99
Unpaved road	300	42.23

By comparing the area with the average LST for LU in. It is clear that green areas and residential use are the lowest in the average temperature, equivalent to 41.02 and 41.09 ℃, respectively. However, their area is small in comparison to the empty areas, paved and unpaved roads, which amounted to 930, 281 and 300 acres, respectively. Their average LST was 42.47, 41.99 and 41.23 ℃,

respectively, which had an effect on raising temperatures in urban space gaps, which amounted to 41.88 ℃ more than the effect of lowering temperatures in residential and green areas. This caused an increase in the average LST of the total urban area, which amounted to 42.11 ℃. This also means UHI elevation of urban area. This difference is clearly shown in Fig. 12.
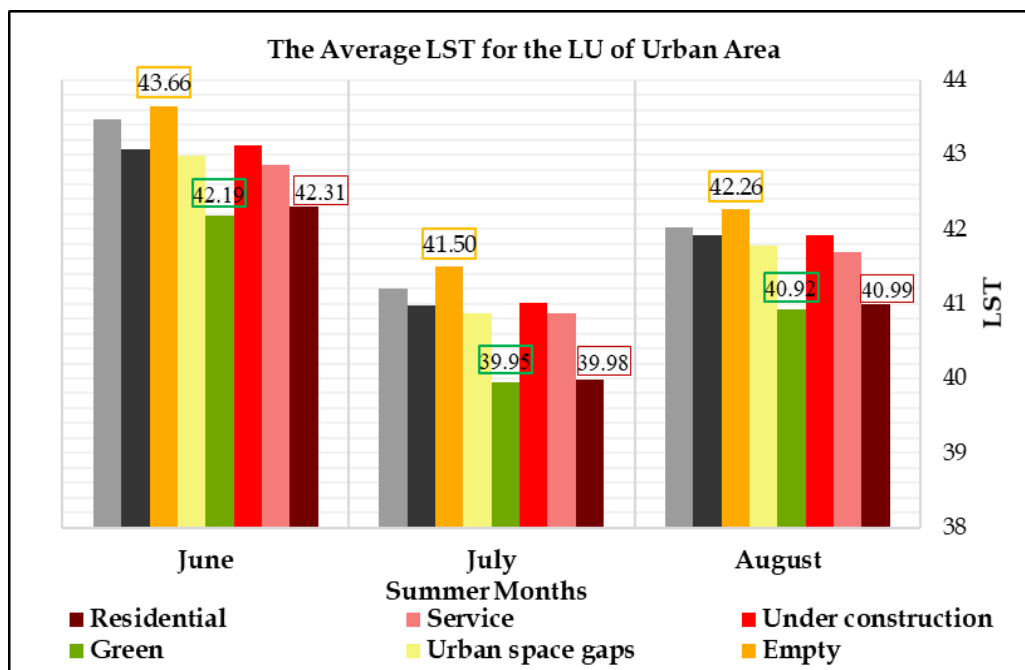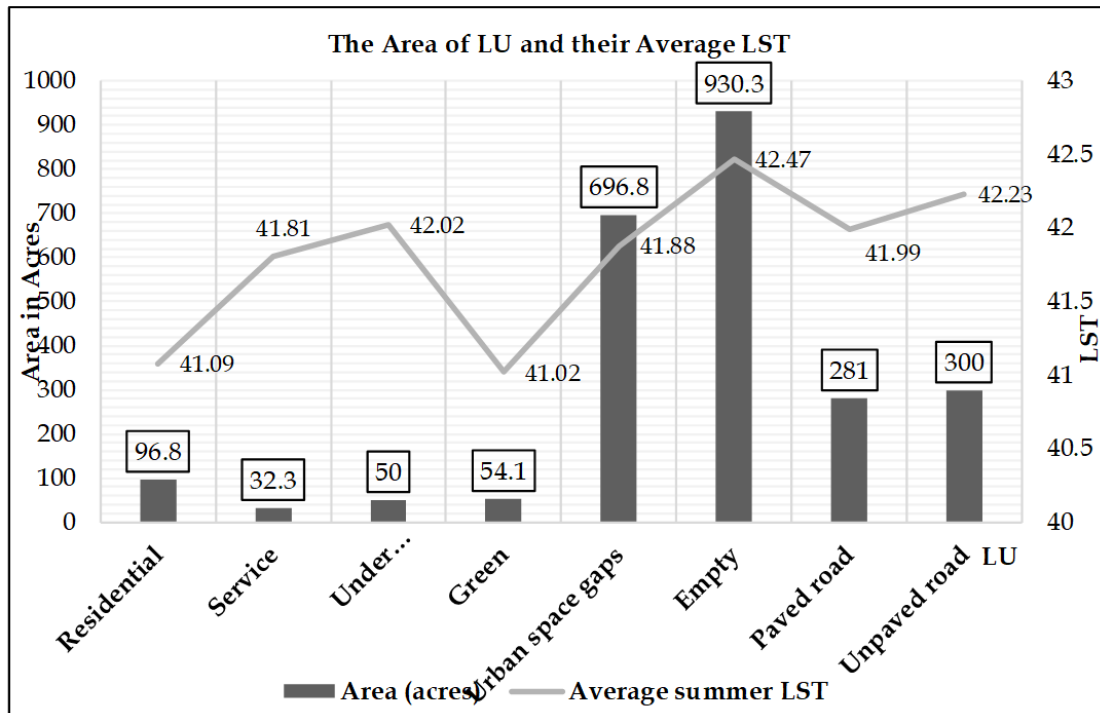
Fig. 11. The average LST for the LU of urban area.

Fig. 12. The area of LU and its average LST during the summer of 2019.

5. Conclusion:

The integration of freely available reference technologies such as RS, GIS and Google Earth helped investigate the effect of LU diversity on the LST. This investigation resulted in some conclusions that can be summarized as follows:

- Residences and green spaces are the places with the lowest average LST.
- Empty areas are the highest in average LST.
- A substantial quantity of solar radiation is absorbed by both paved and unpaved roadways, as well as empty areas, enhancing LST and increasing UHI effect.

As residential areas converge and overlap with green spaces, it is possible that LST for residential use has decreased as a result, which explains the convergence of values between them. This is because the different uses of the city affect each other thermally, through shading, radiation, and thermal conductivity, among other things. Consequently, the less the empty areas and exploited to increase the area of residential uses and green spaces, the lower the average LST of the city, and thus leads to a decrease in the UHI of desert cities. Implying that residential areas and green spaces serve as cold islands in the desert center, just as heat islands do in the rural setting.

References

1. Abdu Yaro, Lawal Abdulrashid, Jerome Ayodele John and Yahaya Sani. 2017. "Remote Sensing and GIS Based Assessment of Urban Heat Island Pattern in Remote Sensing and GIS Based Assessment of Urban Heat Island Pattern in Kaduna Metropolis," no. June.
2. Asgarian, Ali, Bahman Jabbarian Amiri, and Yousef Sakieh. 2015. "Assessing the Effect of Green Cover Spatial Patterns on Urban Land Surface Temperature Using Landscape Metrics Approach." Urban Ecosystems 18 (1): 209–22. https://doi.org/10.1007/s11252-014-0387-7.
3. Bahi, Hicham, Hicham Mastouri, and Hassan Radoine. 2020. "Review of Methods for Retrieving Urban Heat Islands." Materials Today: Proceedings 27: 3004–9. https://doi.org/10.1016/j.matpr.2020.03.272.
4. Bechtel, Benjamin, Klemen Zakšek, and Gholamali Hoshyaripour. 2012. "Downscaling Land Surface Temperature in an Urban Area: A Case Study for Hamburg, Germany." Remote Sensing 4 (10): 3184–3200. https://doi.org/10.3390/rs4103184.
5. Chen, Yanqiu, Baoyan Shan, and Xinwei Yu. 2022. "Study on the Spatial Heterogeneity of Urban Heat Islands and Influencing Factors." Building and Environment 208 (October 2021): 108604. https://doi.org/10.1016/j.buildenv.2021.108604.
6. Ellahham, Nisreen. 2014. "Towards Creating New Sustainable Cities in Egypt-Critical Perspective for Planning New Cities," 1–9.
7. Giannini, M. B., O. R. Belfiore, C. Parente, and R. Santamaria. 2015. "Land Surface Temperature from Landsat 5 TM Images: Comparison of Different Methods Using Airborne Thermal Data." Journal of Engineering Science and Technology Review 8 (3): 83–90. https://doi.org/10.25103/jestr.083.12.
8. Hamdy, Omar, And Shichen Zhao. 2016. "A Study On Urban Growth In Torrent Risk Areas In Aswan, Egypt." Journal Of Architecture And Planning (Transactions Of Aij) 81 (726): 1733–41. Https://Doi.Org/10.3130/Aija.81.1733.

9. Hamdy, Omar, Shichen Zhao, Mohamed A. Salheen, and Youhansen Y. Eid. 2016. "Identifying the Risk Areas and Urban Growth by ArcGIS-Tools." Geosciences (Switzerland) 6 (4). https://doi.org/10.3390/geosciences6040047.

10. Hamdy, Omar, Shichen Zhao, Mohamed A Salheen, and Y Y Eid. 2014. "Using Arc GIS to Analyse Urban Growth towards Torrent Risk Areas (Aswan City as a Case Study)." IOP Conference Series: Earth and Environmental Science 20 (1): 012009. https://doi.org/10.1088/1755-1315/20/1/012009.

11. Haq, Shah Md. Atiqul. 2011. "Urban Green Spaces and an Integrative Approach to Sustainable Environment." Journal of Environmental Protection 02 (05): 601–8. https://doi.org/10.4236/jep.2011.25069.

12. Hegazy, Ibrahim Rizk, and Wael Seddik Moustafa. 2013. "Toward Revitalization of New Towns in Egypt Case Study: Sixth of October." International Journal of Sustainable Built Environment 2 (1): 10–18. https://doi.org/10.1016/j.ijsbe.2013.07.002.

13. Huang, Xinjie, Jiyun Song, Chenghao Wang, Ting Fong May Chui, and Pak Wai Chan. 2021. "The Synergistic Effect of Urban Heat and Moisture Islands in a Compact High-Rise City." Building and Environment 205 (June): 108274. https://doi.org/10.1016/j.buildenv.2021.108274.

14. Ibrahim, Mohamed R., and Houshmand E. Masoumi. 2016. "Will Distance to the Capital City Matter When Supplying New Cities in Egypt?" GeoScape 10 (2): 35–52. https://doi.org/10.1515/geosc-2016-0004.

15. Kulo, Nedim. 2018. "Benefits of the Remote Sensing Data Integration." Conference: 1st Western Balkan Conference on GIS, Mine Surveying, Geodesy and Geomatic, no. December: 0–14. https://www.researchgate.net/publication/329443299_Benefits_of_the_Remote_Sensing_Data_Integration.

16. Li, Zhao-Liang, Bo-Hui Tang, Hua Wu, Huazhong Ren, Guangjian Yan, Zhengming Wan, Isabel F. Trigo, and José A. Sobrino. 2013. "Satellite-Derived Land Surface Temperature: Current Status and Perspectives." Remote Sensing of Environment 131 (April): 14–37. https://doi.org/10.1016/j.rse.2012.12.008.

17. Liu, Shidong, Jianjun Zhang, Jiao Li, Yuqing Li, Jie Zhang, and Xia Wu. 2021. "Simulating and Mitigating Extreme Urban Heat Island Effects in a Factory Area Based on Machine Learning." Building and Environment 202 (March): 108051. https://doi.org/10.1016/j.buildenv.2021.108051.

18. Memon, Rizwan Ahmed, Dennis Y C Leung, and L I U Chunho. 2008. "Review of Generation, Determination, Mitigation UHI." Journal of Environmental Sciences 20: 120–28.

19. Mushore, Terence Darlington, John Odindi, Timothy Dube, Trylee Nyasha Matongera, and Onisimo Mutanga. 2017. "Remote Sensing Applications in Monitoring Urban Growth Impacts on In-and-out Door Thermal Conditions: A Review." Remote Sensing Applications: Society and Environment 8 (August): 83–93. https://doi.org/10.1016/j.rsase.2017.08.001.

20. Mushore, Terence Darlington, John Odindi, Timothy Dube, and Onisimo Mutanga. 2017. "Understanding the Relationship between Urban Outdoor Temperatures and Indoor Air-Conditioning Energy Demand in Zimbabwe." Sustainable Cities and Society 34 (April): 97–108. https://doi.org/10.1016/j.scs.2017.06.007.

21. Osman, T., P. Divigalpitiya, M.M. Osman, E. Kenawy, M. Salem, and Omar. Hamdy. 2016. "Quantifying the Relationship between the Built Environment Attributes and Urban Sustainability Potentials for Housing Areas." Buildings 6 (3). https://doi.org/10.3390/buildings6030039.

22. Ragheb, Ahmed E, and Ayman F Ragab. 2015. "Enhancement of Google Earth Positional Accuracy." International Journal of Engineering Research and Technology 4 (1): 627–30. www.ijert.org.

23. Robbiati, F.O., N. Cáceres, E.C. Hick, M. Suarez, S. Soto, G. Barea, E. Matoff, L. Galetto, and L. Imhof. 2022. "Vegetative and Thermal Performance of an Extensive Vegetated Roof Located in the Urban Heat Island of a Semiarid Region." Building and Environment 212 (October 2021): 108791. https://doi.org/10.1016/j.buildenv.2022.108791.

24. Salem, Esraa Osama, and Miran Essam Monir. 2017. "Policies, Strategies, and Mechanisms of New Cities in Egypt." The Academic Research Community Publication 1 (1): 16. https://doi.org/10.21625/archive.v1i1.115.

25. Salem, Muhammad, Naoki Tsurusaki, Prasanna Divigalpitiya, Taher Osman, Omar Hamdy, Emad Kenawy, Ambra Barbini, Giada Malacarne, Katrien Romagnoli, and Giovanna A Massari. 2020. "Assessing Progress towards Sustainable Development in the Urban Periphery: A Case of Greater Cairo, Egypt." International Journal of Sustainable Development and Planning 15 (7): 971–82.

26. Santamouris, M. 2014. "Cooling the Cities – A Review of Reflective and Green Roof Mitigation Technologies to Fight Heat Island and Improve Comfort in Urban Environments." Solar Energy 103 (May): 682–703. https://doi.org/10.1016/j.solener.2012.07.003.

27. Sekertekin, Aliihsan, and Stefania Bonafoni. 2020. "Land Surface Temperature Retrieval

from Landsat 5, 7, and 8 over Rural Areas: Assessment of Different Retrieval Algorithms and Emissivity Models and Toolbox Implementation." Remote Sensing 12 (2): 294. https://doi.org/10.3390/rs12020294.

28. Shafiee, Elham, Mohsen Faizi, Seyed-abbas Yazdanfar, and Mohammad-ali Khanmohammadi. 2020. "Assessment of the Effect of Living Wall Systems on the Improvement of the Urban Heat Island Phenomenon." Building and Environment 181 (August): 106923. https://doi.org/10.1016/j.buildenv.2020.106923.

29. Stache, E. (Eva), B. (Bart) Schilperoort, M. (Marc) Ottelé, and H.M. (Henk) Jonkers. 2021. "Comparative Analysis in Thermal Behaviour of Common Urban Building Materials and Vegetation and Consequences for Urban Heat Island Effect." Building and Environment, November, 108489. https://doi.org/10.1016/j.buildenv.2021.108489.

30. Stroppiana, Daniela, Massimo Antoninetti, and Pietro Alessandro Brivio. 2014. "Seasonality of MODIS LST over Southern Italy and Correlation with Land Cover, Topography and Solar Radiation." European Journal of Remote Sensing 47 (1): 133–52. https://doi.org/10.5721/EuJRS20144709.

31. Taripanah, Farideh, and Abolfazl Ranjbar. 2021. "Quantitative Analysis of Spatial Distribution of Land Surface Temperature (LST) in Relation Ecohydrological, Terrain and Socio- Economic Factors Based on Landsat Data in Mountainous Area." Advances in Space Research 68 (9): 3622–40. https://doi.org/10.1016/j.asr.2021.07.008.

32. Tran, Duy X., Filiberto Pla, Pedro Latorre-Carmona, Soe W. Myint, Mario Caetano, and Hoan V. Kieu. 2017. "Characterizing the Relationship between Land Use Land Cover Change and Land Surface Temperature." ISPRS Journal of Photogrammetry and Remote Sensing 124 (February): 119–32. https://doi.org/10.1016/j.isprsjprs.2017.01.001.

33. Ulfiasari, Sofi, and Lin Yola. 2022. "How Does Urban Development Contributes to Urban Heat Island: A Decade Increase of Urban Heat Intensity in Jakarta Metropolitan Area." In Lecture Notes in Civil Engineering, 161:67–77. https://doi.org/10.1007/978-981-16-2329-5_9.

34. Unal Cilek, Muge, and Ahmet Cilek. 2021. "Analyses of Land Surface Temperature (LST) Variability among Local Climate Zones (LCZs) Comparing Landsat-8 and ENVI-Met Model Data." Sustainable Cities and Society 69 (October 2020). https://doi.org/10.1016/j.scs.2021.102877.

35. Voogt, J.A, and T.R Oke. 2003. "Thermal Remote Sensing of Urban Climates." Remote Sensing of Environment 86 (3): 370–84.

https://doi.org/10.1016/S0034-4257(03)00079-8.

36. Wang, Qun, Cheng Zhang, Chao Ren, Jian Hang, and Yuguo Li. 2020. "Urban Heat Island Circulations over the Beijing-Tianjin Region under Calm and Fair Conditions." Building and Environment 180 (August): 107063. https://doi.org/10.1016/j.buildenv.2020.107063.

37. Weng, Qihao. 2009. "Thermal Infrared Remote Sensing for Urban Climate and Environmental Studies: Methods, Applications, and Trends." ISPRS Journal of Photogrammetry and Remote Sensing 64 (4): 335–44. https://doi.org/10.1016/j.isprsjprs.2009.03.007.

38. Wu, Caiyan, Junxiang Li, Chunfang Wang, Conghe Song, Dagmar Haase, Jürgen Breuste, and Maroš Finka. 2021. "Estimating the Cooling Effect of Pocket Green Space in High Density Urban Areas in Shanghai, China." Frontiers in Environmental Science 9 (May): 1–14. https://doi.org/10.3389/fenvs.2021.657969.

39. Yang, Chaobin, Xingyuan He, Ranghu Wang, Fengqin Yan, Lingxue Yu, Kun Bu, Jiuchun Yang, Liping Chang, and Shuwen Zhang. 2017. "The Effect of Urban Green Spaces on the Urban Thermal Environment and Its Seasonal Variations." Forests 8 (5): 1–19. https://doi.org/10.3390/f8050153.

40. Yin, Jie, Xiaoxu Wu, Miaogen Shen, Xiaoli Zhang, Chenghao Zhu, Hongxu Xiang, Chunming Shi, Zhiyi Guo, and Chenlu Li. 2019. "Impact of Urban Greenspace Spatial Pattern on Land Surface Temperature: A Case Study in Beijing Metropolitan Area, China." Landscape Ecology 34 (12): 2949–61. https://doi.org/10.1007/s10980-019-00932-6.

41. Youssef, Ahmed M., Biswajeet Pradhan, and Elhami Tarabees. 2011. "Integrated Evaluation of Urban Development Suitability Based on Remote Sensing and GIS Techniques: Contribution from the Analytic Hierarchy Process." Arabian Journal of Geosciences 4 (3–4): 463–73. https://doi.org/10.1007/s12517-009-0118-1.

42. Yu, Xiaolei, Xulin Guo, and Zhaocong Wu. 2014. "Land Surface Temperature Retrieval from Landsat 8 TIRS—Comparison between Radiative Transfer Equation-Based Method, Split Window Algorithm and Single Channel Method." Remote Sensing 6 (10): 9829–52. https://doi.org/10.3390/rs6109829.

43. Zhang, Li, Xiaochun Yang, Yue Fan, and Jiahao Zhang. 2021. "Utilizing the Theory of Planned Behavior to Predict Willingness to Pay for Urban Heat Island Effect Mitigation." Building and Environment 204 (July): 108136. https://doi.org/10.1016/j.buildenv.2021.108136.

44. Zou, Zhendong, Chunhua Yan, Leiyu Yu, Xianchenghao Jiang, Jinshan Ding, Longjun Qin, Bei Wang, and Guoyu Qiu. 2021. "Impacts

of Land Use/ Land Cover Types on Interactions between Urban Heat Island Effects and Heat Waves." Building and Environment 204 (July): 108138. https://doi.org/10.1016/j.buildenv.2021.108138.

45. Al-Jashami, Samer Hadi Kazem. 2018. "Spatial Analysis of Heat Islands in the City of Najaf Using Geographical Techniques." Journal of Geographical Research 27 (1): 327–54. https://doi.org/10.36328/0833-000-027-012.

46. USGS. n.d. "EarthExplorer." Accessed August 25, 2021. https://earthexplorer.usgs.gov/.

47. "New Urban Communities Authority, Home Page - New Tiba." n.d.